Early development of the malleus and incus in humans

Burford, Charlotte M. [1]

Mason, Matthew J. [2]

University of Cambridge

Department of Physiology, Development & Neuroscience

Downing Street

Cambridge CB2 3EG

1. Current address:

Faculty of Life Sciences & Medicine,

King's College London,

London, SE1 1UL

2. Corresponding author

Abstract

It is widely accepted by developmental biologists that the malleus and incus of the mammalian middle ear are first pharyngeal arch derivatives, a contention based originally on classical embryology which has now been backed up by molecular evidence from rodent models. However, it has been claimed in several studies of human ossicular development that the manubrium of the malleus and long process of the incus are actually derived from the second arch. This 'dual-arch' interpretation is commonly presented in otolaryngology textbooks, and it has been used by clinicians to explain the aetiology of certain congenital abnormalities of the human middle ear.

In order to re-examine the origins of the human malleus and incus, we made 3D reconstructions of the pharyngeal region of human embryos from 7 to 28 mm crown-rump length, based on serial histological sections from the Boyd Collection. We considered the positions of the developing ossicles relative to the pharyngeal pouches and clefts, and the facial and chorda tympani nerves. Confirming observations from previous studies, the primary union between first pharyngeal pouch and first cleft found in our youngest specimens was later lost, the external meatus developing rostroventral to this position. The mesenchyme of the first and second arches in these early embryos seemed to be continuous but the boundaries of the developing ossicles proved to be very hard to determine at this stage. When first distinguishable, the indications were that both the manubrium of the malleus and the long process of the incus were emerging within the first pharyngeal arch. We therefore conclude that the histological evidence, on balance, favours the 'classical' notion that the human malleus and incus are first-arch structures. The embryological basis of congenital ossicular abnormalities should be reconsidered in this light.

Keywords

Embryology, development, malleus, incus, pharyngeal arch

Introduction

The development of the auditory ossicles of mammals has attracted considerable attention over the years, not least because of the contribution of embryological studies to our knowledge of the evolution of the malleus and incus from the jaw-bones of our tetrapod ancestors (Reichert, 1837; Gaupp, 1913). The malleus has a composite structure: most of it is formed from endochondral bone but the goniale, which will form its anterior process, is an intramembranous ossification which develops separately from the rest of the ossicle (Hanson & Anson, 1962; Rodríguez Vázquez *et al.*, 1991; Tucker *et al.*, 2004). The endochondral component of the malleus and all of the incus develop from pharyngeal arch cartilage, of neural crest origin. Most of the stapes also develops from pharyngeal arch cartilage but the outer edge of its footplate has a mesodermal origin, at least in mice (Thompson *et al.*, 2012).

In the nineteenth and early twentieth centuries, the developmental origins of the auditory ossicles were much debated (reviewed by Gaupp, 1913; Strickland *et al.*, 1962). Opinion slowly condensed around Reichert's (1837) concept that the malleus and incus develop from pharyngeal arch I (mandibular arch) cartilage, while the stapes is derived from pharyngeal arch II (hyoid arch) cartilage. This conclusion, referred to here as the "classical interpretation" (Fig. 1), was originally based on evidence from dissections and histological sections but it has been supported by the results of more recent experiments on mice. Mice with homozygous *Hoxa2* gene mutations lack second-arch structures including a stapes, but instead exhibit duplication of first-arch structures including Meckel's cartilage, malleus and incus (Gendron-Maguire *et al.*, 1993; Rijli *et al.*, 1993). Notably, the manubrium of the malleus and the long process of the incus are present in the mutant mice, in both cases fused to their respective duplicated versions (Rijli *et al.*, 1993). In a fate-mapping study of mouse ear development, O'Gorman (2005) found that nearly all of the endochondral malleus and all of the incus are derived from first-arch cartilage. Only one, short process near the base of the manubrium of the malleus was found to be of second-arch origin. This process was originally identified as the 'processus brevis', another term for the lateral process of the human malleus (Fig. 1). However, this second-arch process in the mouse malleus actually appears to be the orbicular apophysis, a structure which is not found in the human malleus (Mason, 2013). The origin of the orbicular apophysis notwithstanding, the "classical interpretation" that the malleus and incus are essentially first-arch structures has been widely accepted in recent studies of rodent ear development (see e.g. Matsuo *et al.*, 1995; Miyake *et al.*, 1996; Mallo, 1997; Mallo *et al.*, 2000; Amin & Tucker, 2006; Kitazawa *et al.*, 2015), reviews of middle ear development and evolution (Chapman, 2011; Luo, 2011; Anthwal *et al.*, 2013; Sienknecht, 2013; Anthwal & Thompson, 2016) and at least one clinical textbook (Gleeson *et al.*, 2008).

There remains, however, a competing hypothesis regarding the developmental origins of the malleus and incus which, while agreeing that the bodies of the ossicles arise in the first arch, maintains that the manubrium of the malleus and the long process of the incus are actually second-arch structures (Fig. 1). This will be referred to here as the "dual-arch interpretation". In his influential treatise on middle ear evolution, Gaupp (1913) considered some earlier studies by Hammar and Fuchs in which such a notion had been proposed, but he did not regard the evidence as reliable. The dual-arch interpretation faded into obscurity, re-emerging much later with the work of Barry J. Anson's group (Hanson *et al.*, 1959; Anson *et al.*, 1960; Hanson *et al.*, 1962; Strickland *et al.*,

1962), of which Hanson et al. (1962) represents the definitive paper. Having examined serial sections of human embryos from 7 to 28 mm crown-rump length (CRL), Hanson et al. based their conclusions on two key observations. Firstly, the blastemal mass which will become malleus and incus was found in a 9.6 mm CRL embryo to extend above and below the first pharyngeal cleft, and was thus held to originate from both arches I and II. By comparison with later embryonic stages, the bodies of the malleus and incus were taken to develop in the first-arch component of this blastemal mass, while the manubrium and long process were taken to develop in the second-arch component. Hanson et al. (1962) emphasized the importance of looking at precartilaginous (i.e. mesenchymal) developmental stages of the auditory ossicles in order to elucidate their pharyngeal arch origin, because the manubrium and long process were found to separate from the rest of the second arch tissue very early (around the 11.7 mm stage). Their second observation concerned their finding that in 30 of 198 normal specimens, ranging from embryo to adult, the stapedius muscle tendon inserted onto the incudal long process, as well as onto the stapes.

Presley (1984) examined embryos from a number of different mammalian species and could not corroborate the findings of the Anson group, but more recent papers focusing specifically on human embryology have supported the dual-arch interpretation. Ars (1989) agreed that the manubrium and long process are second-arch structures, but this may not have been based on original observations. Louryan (1993) based his support on the independent examination of sections of human embryos from 9 to 27.5 mm CRL; a textbook co-authored by Louryan later pictured a section of a 13 mm embryo to reinforce this notion (Mansour *et al.*, 2013). Whyte et al. (2009) also supported a dual-arch origin based on their examination of human embryonic sections, but their description of the long process and manubrium fusing with the ossicular bodies at the cartilaginous stage, around 27 mm CRL, is very different to the much earlier process of mesenchymal separation described by Hanson's group. The dual-arch interpretation was presented in the form of a figure in the 37th, 38th and 39th editions of *Gray's Anatomy* (Williams *et al.*, 1989; Williams *et al.*, 1995; Standring *et al.*, 2005), although apparently not in previous or subsequent editions, and it is the view put forward in several recent otology textbooks (Gopen, 2013; Bluestone *et al.*, 2014; Pasha & Golub, 2014). Many clinicians have based their aetiological interpretations of various developmental abnormalities of the middle ear in terms of a dual-arch origin of the malleus and incus (see Discussion).

Other hypotheses regarding the origins of the mammalian ossicles have also been suggested. Dissatisfied with the evidence supporting the classical interpretation, Jarvik (1980) and Otto (1984) independently proposed that the malleus and incus are entirely second-arch structures. Their interpretations, which require that the embryonic connection between malleus and Meckel's cartilage is a secondary union, have not attracted support, but it is interesting to note that one of the reconstructions made by Hanson et al. (1962) was used as part of Otto's case.

There are, then, competing hypotheses relating to the pharyngeal arch origins of the malleus and incus. Recent support for the classical interpretation has come predominantly from experimental studies of laboratory rodents, while the human anatomical and clinical literature tends to favour the dual arch interpretation. Another aspect of ear development forms an interesting parallel: the mesenchyme contributing to the mouse pinna has recently been found to come from the second pharyngeal arch only, while a dual-arch origin is commonly held to be the case in the human literature (Minoux *et al.*, 2013).

The aim of the present study was to reassess the evidence put forward by Hanson et al. (1962) and Whyte et al. (2009) in favour of their different versions of the dual-arch interpretation. Because these concepts emerged from examinations of histological sections of human embryos, it seemed appropriate to look at similar material in order to verify their claims.

J. Dixon Boyd (1907-1968), most famous for his work on human development, was Professor of Anatomy at the University of Cambridge from 1951 until his death. Boyd's vast collection of embryological slides, which remains in the University of Cambridge, proved to include a large number of sectioned embryos of the right size-range from which we could make three-dimensional computer reconstructions. Because we needed to establish the position of the ossicular precursors relative to the pharyngeal pouches and clefts, it was necessary to consider the early development of the middle ear cavity and external meatus as well as the ossicles themselves. Hanson et al. (1962) found that the facial nerve and its chorda tympani branch come to separate the malleus and incus primordia from the second branchial bar, the chorda tympani later dividing the primordia of the manubrium and the incudal long process. These nerves therefore represent useful landmarks for the identification of the ossicular precursors, so they were also reconstructed.

Materials and Methods

Histological serial sections from 47 embryos were examined in this study, all from the Boyd Collection (see Supplemental Table 1). Crown-rump lengths were from 7 to 33.5 mm. These embryos were considered to represent Carnegie stages 14 to 23, and were likely aged between 1 and 2 months post-fertilization. Most of them had been collected in the 1950s and early 1960s from hospitals in the east of England, often following hysterectomies or abortions; some were ectopic. Other examined sections in the Boyd Collection appeared to be much older. Information relating to the processing of the embryos was scanty. Fixation was typically based on formalin and/or Bouin's fluid. The embryos had been sectioned at thicknesses from 5 to 15 μm; those sectioned in the transverse plane were found to be the most useful for the purposes of this study. Staining techniques included haematoxylin & eosin, Masson's trichrome, periodic acid-Schiff and Bodian's method. In many cases, sections from the same embryo series had been stained in a variety of unspecified ways.

3D reconstructions were made from 32 embryos (7 to 28 mm CRL). Sections from these embryos were photographed using a GXCAM-5 digital camera fitted to a Motic SMZ-168 light microscope. Images were captured as high-resolution .tiff files using GXCapture 8.0 (GT Vision Ltd.) software. Individual files were then reduced in size by conversion to jpeg format and, in most cases, greyscale by IrfanView 4.37 (Irfan Skiljan, 2014). ImageJ 1.45 s (W. Rasband, 2011, National Institutes of Health), running the Stackreg plugin (Thévenaz 2011, Biomedical Imaging Group, Swiss Federal Institute of Technology, Lausanne; see Thévenaz *et al.*, 1998), was used to align the sequence of images, using a recursive procedure based on rigid-body translation and rotation. If an obvious registration error occurred, evident as a 'jump' in the aligned sequence, this was manually corrected by translating and rotating the problematic sections in Adobe Photoshop CS 8.0 (Adobe Systems Inc.,

2003). Three-dimensional reconstructions were then made from the aligned image stack using WinSurf 4.0 (Moody & Lozanoff, 1998). This required manual highlighting of the anatomical borders of key structures in a subset of the aligned sections. Structures which were reconstructed in this way included the skin of the head and external meatus, pharyngeal pouches, facial nerve, chorda tympani and pharyngeal arch mesenchyme or cartilage.

Slides of particular interest were photographed at higher magnification using the same camera fitted to a Leitz HM-LUX light microscope. Images were laterally inverted where necessary, to facilitate comparison.

All embryo sizes are given as crown-rump lengths (CRL), as recorded in the Boyd Collection archive. For the purposes of orientation, *rostral* is used here to indicate the direction towards the nose; *caudal* is the opposite direction. *Dorsal* indicates the direction towards the crown of the head; *ventral* is the opposite. The rostro-caudal and dorso-ventral axes are orthogonal.

Results

General points

Although there was a clear relationship between CRL and stage of pharyngeal development, the correlation was not perfect: for example, one 14 mm embryo (H241) was found to be at a more advanced stage of development than a 17 mm embryo (H25). Therefore, rather than categorizing embryos by length, the examined embryos are grouped here into seven middle ear developmental stages, A-G. Clearly, embryos fall within a developmental spectrum and structures do not always develop at the same relative rates, so there were small differences between embryos of any given stage.

Stage A, 7-9 mm CRL

In the smallest embryos examined, four pharyngeal arches were apparent (Fig. 2, 3A). The mandibular and hyoid arches form prominent external swellings, divided by the deep groove representing cleft I. Pouch I projects in a caudolateral direction from the pharynx, towards the caudal end of cleft I. Below the bulge of the second arch is a shallow invagination of the side of the head which will become the cervical sinus. Cleft II extends inwards from the sinus towards pouch II; just below this is a combined cleft extending towards pouches III and IV. Pouches II, III and IV project ventrolaterally and rostrally from the pharynx, with which they are in free communication. Pouches III and IV are small but well-developed. No fifth pouch was observed.

Pharyngeal pouches I-IV closely approach their respective clefts, pouch and cleft being separated only by a thin layer of cells which appeared to be endodermal and/or ectodermal in origin (Fig. 3B). In some cases, this cellular division had broken down such that the pouch was in free communication with the external environment by means of a narrow channel. Away from the point of contact between pouch and cleft, mesenchyme is interposed between the pouch endoderm and cleft ectoderm. However, in the region caudal to the chorda tympani, a pale line marking a slight separation between dorsal and ventral blocks of mesenchymal cells could sometimes be seen

extending between pouch I and cleft I (Fig. 2). From their relative positions, these mesenchymal blocks appeared to represent arch I and arch II contributions, respectively. A similar pale line was seen dividing the mesenchyme of arches II and III, centrally.

The mesenchyme within pharyngeal arches I and II is very diffuse at this stage: with the exception of the pale lines referred to above, boundaries could not be reliably distinguished (Fig. 5A, 6A).

Stage B, 9.5-11 mm CRL

Pharyngeal pouches I and II remain intimately apposed to, or in some cases in open communication with, their respective clefts. Pouches III and IV, however, have separated from their combined cleft. Mesenchyme remains very diffuse, but in the more advanced embryos of this stage, mesenchyme in the arch II region is just beginning to condense in the future stapes region (Fig. 4A) and more rostrally in what will become the central part of Reichert's cartilage (Fig. 2). As in stage A embryos, a pale line appearing to divide arch I and arch II mesenchyme is visible in some sections, extending between pouch I and cleft I (Fig. 4B).

Stage C, 10-15 mm CRL

Pouch I narrows laterally as it approaches the caudal part of cleft I: mesenchyme is now interposed between endoderm and ectoderm but pouch and cleft remain in very close proximity (Fig. 3C, D). Pouch II tapers rapidly as it emerges from the pharynx, and it too separates from its cleft. Pouches III and IV are very small; pouch III loses its connection to the pharynx.

In the region just rostral to the tip of pouch I, a band of mesenchymal cells appears to run uninterrupted between first- and second-arch regions, sandwiched between cleft I laterally and the base of pouch I medially (Fig. 6B). At its dorsal end, within arch I territory, this band widens out into a cloud of cells from which will form the short process and body of the incus. Ventrally, the band reaches the slightly more condensed mesenchyme wrapping around the dorsal aspect of the facial nerve, in arch II territory. This mesenchymal bridge between arch I and arch II is in the region where the long process of the incus will develop, but at this stage the cells here remain relatively loose and the process itself cannot yet be distinguished.

A little more rostrally, towards the origin of the chorda tympani from the facial nerve, the bridging mesenchymal band appears to be divided by the very narrow, pale line which extends between pouch I and cleft I, described earlier. This division is clearer in some embryos than in others. Two condensations are visible within the relatively loose mesenchyme, above and below this dividing line. The lower condensation, on the medial side of the facial nerve, forms a dense, mesenchymal rod which runs medially from here within arch II territory: this is Reichert's bar (Fig. 2, 5B). The upper condensation, less well-defined but clearly separated from Reichert's bar, will form the malleus and manubrium (Fig. 5B). Meckel's bar, projecting rostrally from the malleus, is also beginning to develop.

The stapes begins to appear as a dense, oval condensation of mesenchymal cells between the rostral otic capsule and the facial nerve. The bulk of the stapes, which lies between this and Reichert's bar, is still made up of very loose mesenchyme and is hence much more difficult to discern, but a rounded mass can just be made out, through which the stapedial artery passes. Its boundaries remain unclear, especially laterally and ventrally, but it is constrained rostrally and dorsally by the first pharyngeal pouch.

Stage D, 13.5-17 mm CRL

The first pouch is now widely separated from the first cleft, by mesenchyme. The narrow, distal parts of pouches I and II have disappeared and the two pouches are no longer distinct. Their confluent bases form a wing-like evagination, on either side of the pharynx. The rostroventral part of cleft I is invaginating further: this invagination will become the external auditory meatus. The other clefts have effectively disappeared. Pouches III and IV are now vestigial; pouch IV cannot be found in some embryos. The fates of these pouches will not be pursued further.

The mesenchyme from which the malleus and incus are constructed is still relatively loose and the ossicles cannot be separated, but their combined boundaries are becoming clearer. The short process of the incus is dorsal, lateral and now somewhat caudal to the lateral extent of the pharyngeal 'wing'. Closer to the 'wing', the long process is just distinguishable (Fig. 6C), extending downwards towards the stapes. The tip of the long process appears to be narrowly separated from the stapes by a band of looser mesenchyme. Rostral to the long process, the malleo-incudal mesenchyme retreats dorsally and then extends downwards again as the manubrium of the malleus, a blunt, mesenchymal mass located between the pharyngeal 'wing' and cleft I (Fig. 5C). The chorda tympani nerve runs across the manubrium, between this and the long process of the incus. The head of the malleus is continuous with Meckel's bar, which becomes much more definite in its outline centrally, where a dense, mesenchymal perichondrium surrounds a precartilaginous core. The distal end of Meckel's bar is still mesenchymal, and it does not yet meet its contralateral counterpart.

The distal end of Reichert's bar reaches the developing laryngeal cartilages, almost at the midline. Proximally, Reichert's bar wraps around the dorsal surface of the facial nerve, narrowing as it does so. This part of the second-arch condensation, which remains mesenchymal at this stage, bifurcates into an indistinct lateral projection and a short dorsal branch, which is continuous with the stapes. Using terminology based on the careful description of Rodríguez-Vázquez (2009), the lateral projection represents the laterohyale while the dorsal branch is the interhyale, the precursor of the stapedius tendon. The stapes itself is an ovoid mass, made of less dense mesenchyme than Reichert's bar but now with distinguishable boundaries. The narrow stapedial artery passes through the centre of this mass, through a foramen at this stage little wider than the artery itself.

Stage E, 14-18 mm CRL

The pharyngeal pouch/cleft arrangement in these embryos (Fig. 2, 3F) shows little advance over stage D. However, the future articulation zone between malleus and incus has become demarcated as dense mesenchyme. The articulation between the long process of the incus and the stapes is also clearer, these two ossicular precursors remaining very narrowly separated. The malleus head, incus head and Reichert's bar are precartilaginous (Fig. 5D, 6D), as is the stapes. The tensor tympani muscle can just be discerned, between the malleus and pharyngeal 'wing'.

Stage F, 20-22 mm CRL

The pharyngeal 'wing' has elongated laterally and may now be described as the tubotympanic recess. The incipient external meatus is longer and narrower. The manubrium is growing downwards within the narrowing layer of mesenchyme sandwiched between the recess and meatus.

The ossicles have further consolidated such that their boundaries are very clear (Fig. 5E, 6E); the same is true of the otic capsule which has developed around the endolymphatic channels. The proximal parts of the manubrium and the long process of the incus are chondrifying. Meckel's bar is

now cartilaginous to its distal end, which is slightly expanded and almost touching its contralateral counterpart in the region of the future mandibular symphysis. The short process of the incus and the laterohyale abut the cartilaginous otic capsule.

Stage G, 24-28 mm CRL

The external meatus remains relatively long and narrow, its internal end becoming cup-shaped as it approaches the manubrium. The tubotympanic recess has elongated further: proximally, its connection to the pharynx proper has become relatively narrow, this representing the beginnings of the Eustachian tube.

The manubrium, which is elongating but still relatively stubby (Fig. 5F), pushes into the flared distal end of the tubotympanic recess. Its tip remains mesenchymal. Meckel's cartilage is indistinguishable from the rest of the malleus in almost all stage G embryos (Fig. 5F, 7B-D). However, in one 28 mm embryo (H983), the Meckel's cartilage component of the malleus head is partially separated from the neck and manubrium by a thin line of dark mesenchyme (Fig. 7A). The same line of division is present on both left and right mallei, and did not appear to be a shrinkage artefact.

Both the short process of the incus and that part of Reichert's cartilage which will become the styloid process are now fused with the cartilaginous otic capsule. The incudal long process is cartilaginous to its tip (Fig. 6F), but there is not yet a lenticular apophysis. The stapedius muscle has attained a clear identity. A pale halo, which presumably marks the site of the future annular ligament, separates the stapes footplate from from the oval window.

Embryos of 29-33.5 mm were not examined in such detail, but their ossicles appeared similar to those of the stage G embryos.

Discussion

The development of the middle ear cavity and external meatus

A summary of what the present study has revealed regarding the development of the pharynx, tubotympanic recess and ossicles is presented in diagrammatic form as Figure 8. The original pharyngeal extensions forming the first and second pouches are distinct in the earliest embryos examined and contact their respective clefts (Fig. 3A, B). In some cases, there was no dividing membrane between pouch and cleft, such that the pharynx was in direct continuity with the external environment. The first pouch is originally directed caudolaterally, the second in the ventro-rostro-lateral direction; they share a broad base. However, the two narrow extensions lose their primary contacts with their respective clefts, the epithelia becoming separated by an interposed layer of mesenchyme (Fig. 3C, D). The extensions either regress, or perhaps are outpaced in their lateral growth, by the wing-like pharyngeal evagination which seems to emerge from the broad base of the two pouches to become the tubotympanic recess. The relative contributions of pouch I and pouch II endoderm to the tubotympanic recess in humans have been debated (Frazer, 1914; Kanagasuntheram, 1967). In the present study, it proved impossible to judge the extent that each pouch contributed to the wing-like evagination, and so no further light could be shone on this issue.

The original contact between pouch I and cleft I was at the caudodorsal end of the first cleft, but the external auditory meatus appears later as an invagination towards the rostroventral end of the cleft (Fig. 3C, E-G). The meatus converges with the distal end of the tubotympanic recess, the narrowing layer of mesenchyme which remains in-between ultimately contributing to the tympanic membrane. The tympanic membrane therefore develops not at the original, spiracular union between pouch I and cleft I, but at a later, secondary contact between tubotympanic recess and external meatus. The transient nature of the original contact between pouch I and cleft I is described in the literature (see e.g. Presley, 1984) but has often been overlooked in recent textbooks and articles. Apparently surprised to find that the external meatus of mice did not form at the original pouch I-cleft I union, Minoux et al. (2013) demonstrated that the meatus in this species invaginates into *Hoxa2*-negative mesenchyme, presumed to be entirely of first-arch origin.

The development of the malleus and incus

The mesenchymal stage

According to the Anson group (Hanson *et al.*, 1959; Anson *et al.*, 1960; Hanson *et al.*, 1962; Strickland *et al.*, 1962), the first- and second-arch components of the malleus and incus are distinguishable only at the mesenchymal stage. Hanson et al. (1962) argued that in their 9.6 mm embryo, the blastemal mass from which both malleus and incus will condense consists of continuous arch I and arch II mesenchyme. They used the position of "branchial groove I", the first pharyngeal cleft, to distinguish between the first-arch and second-arch contributions to this mass. According to these authors, the malleus and incus bodies form in the arch I mesenchyme above the groove, whereas the manubrium and long process form in arch II mesenchyme below the groove. The facial nerve and chorda tympani later divide the manubrium and incudal long process from the rest of the second arch mesenchyme, which will form the stapes, styloid process and other structures. Louryan (1993) largely agreed with these findings, but implied that the manubrium develops separately from the rest of the malleus.

In many of the early embryos (stages A-C) examined here, what appeared to be a partial division of first and second-arch mesenchyme was visible in some sections, extending between pouch I and cleft I (Fig. 4B). The bodies of the malleus and incus form above this dividing line, and clearly represent arch I structures (in agreement with both the classical and dual-arch interpretations, which do not differ on this point). Just caudal to this region, where the long process develops (Fig. 4A), and just rostral to it, where the manubrium develops (Fig. 4C), the first and second-arch mesenchyme appeared to be continuous. The long process and manubrium could, then, potentially be derived from arch II mesenchyme, as per the dual-arch interpretation. However, the cells contributing to these structures could equally have arisen in arch I and pushed downwards from there. Frazer (1914) and Kanagasuntheram (1967) both described the mesenchyme which will form the human manubrium as extending from the first arch region; Kanagasuntheram examined embryo sections obtained from J.D. Boyd, possibly including some of the same ones examined in the present study. Miyake et al. (1996), looking at early mouse embryos, found that the caudal part of the first-arch chondrogenic condensation which will develop into the incus and part of the malleus was actually located in hyoid arch territory, but this was separate from the second-arch condensations which would go on to form the stapes and Reichert's cartilage.

At the point where the long process of the incus was beginning to condense and could be identified (around stage D), it appeared to be continuous with the incudal body above (in arch I), but narrowly separated from the stapes below (in arch II). Similarly, the developing manubrium was continuous with the malleus body above (arch I) but separate from Reichert's cartilage below (arch II). We therefore found no evidence to suggest that the manubrium forms separately from the rest of the malleus. It was very difficult to define boundaries of these structures in these early embryos, but it was not clear from our reconstructions that either the manubrium or the long process, when first identifiable, extended below cleft I. We therefore feel that, on balance, the histological evidence regarding the origins of manubrium and long process favours the classical interpretation.

The malleus and Meckel's bar appear to condense out of the same diffuse mesenchymal mass, around stage C. Although their condensation and later conversion to cartilage does not proceed synchronously along the whole length of the combined structure, we found no clear evidence to suggest that these are developmentally separate entities which later fuse, contrary to the hypotheses put forward by Jarvik (1980) and Otto (1984).

The cartilaginous stage

Whyte et al. (2009) claimed that the manubrium of the malleus and the long process of the incus are separate from the bodies of these ossicles in the cartilaginous embryonic stages, the processes fusing with the bodies in human embryos of around 27 to 30 mm CRL. In the present study, with the single exception of H983, discussed below, the manubrium was always continuous with the body of the malleus and the long process of the incus was always continuous with the rest of the incus. The manubrium was very short and stubby to begin with, extending distally as the embryos got larger. Chondrification proceeded from proximally to distally along both processes such that the tips remained mesenchymal for longest. Chondrification of the mouse manubrium is believed to require signals from the developing external meatus (Mallo *et al.*, 2000). As mentioned earlier, the meatus invaginates into and is completely surrounded by what appears to be first-arch mesenchyme (Minoux *et al.*, 2013).

In the sections made from one 28 mm human embryo (H983), a thin dividing line of dense mesenchyme appeared to separate that part of the malleus which is directly continuous with Meckel's cartilage, including the head region, from the lower parts of the malleus, including the manubrium (Fig. 7A): this was the case in both right and left ears. There was no visible division of the incudes. None of the 19 other examined embryos from 24-33.5 mm CRL showed any signs of division within either ossicle (see Fig. 5F, 7B-D). H983 had been sectioned in a slightly different plane to the others, which largely accounts for the difference in malleus shape between this and the other ossicles visible in Figure 7, but neither this nor the shrinkage artefacts visible in other H983 sections could obviously account for the presence of this intra-mallear division.

In support of their version of the dual-arch interpretation, Whyte et al. (2009) presented a single photomicrograph of a 27 mm embryo which was said to show the processes beginning to fuse with the bodies of the ossicles. Their photomicrograph does not resemble what we observed in H983, and we believe that it was in fact misinterpreted. In our reinterpretation, what was labelled by Whyte et al. as the head of the malleus is actually the head of the incus, and the region interpreted as a zone of fusion between this and the manubrial neck is part of the malleo-incudal articulation. We believe that the region interpreted as a zone of fusion between the incudal long process and the incudal

body is simply the result of the section plane skimming the edge of where these structures are in continuity.

The orbicular apophysis ('processus brevis') of mice

Takechi & Kuratani (2010) suggested that the differences of opinion regarding the pharyngeal arch origins of the human malleus and incus might be resolved in the light of what O'Gorman (2005) found in his fate-mapping study of mouse middle ear development. Although the bulk of the malleus (including the manubrium) and all of the incus were found to be first-arch structures, O'Gorman found that the 'processus brevis' of the mouse malleus comes from the second arch. Takechi & Kuratani implied that the second-arch mesenchyme identified by dual-arch proponents as the manubrium of the malleus might instead become this 'processus brevis'. However, Mason (2013) showed that the 'processus brevis' of the mouse is in fact the orbicular apophysis, a process characteristic of the mouse malleus which is not found in humans. No trace of the orbicular apophysis was found in developing human ossicles in the present study, and it is concluded that this is not the basis of the dual-arch interpretation.

The stapedius muscle insertion

Hanson et al. (1959; 1962) found fibres of the stapedius muscle tendon inserting on the distal tip of the long process of the incus in 15% of the specimens examined, which ranged in age from embryo to adult. This connection was used by these authors as further evidence supporting a second-arch origin of the long process. In fact, it is not clear from the photomicrographs of a 21-week fetus and a neonate presented by Hanson et al. (1959) in support of their observation that the tendon is actually inserting on the incus and not onto the incudostapedial joint capsule. The well-developed joint capsule envelops the stapes head, the lenticular apophysis of the incus and the pedicle connecting the apophysis to the distal long process, and it contains both collagenous and elastic fibres (Chien *et al.*, 2009). The stapedius tendon was found to insert into the joint capsule as well as the stapes head in 7 of 103 human specimens examined by Chien et al. (2009), ranging in age from neonate to 100 years. A distinct stapedial insertion on the incus was not observed in any of the embryonic specimens examined in the present study.

Although they believed that the long process of the incus has a second-arch origin, Hanson et al. (1962) noted that the connection between long process and stapes is a *secondary* union. At around the 11.7 mm stage they found that the long process "swings toward the stapedial ring to fuse with the future head of the stapes; thus, a secondary continuity is established between the structures within the first and second branchial arches" (p.208). No 'swinging' of the long process was observed in the present study, but at the point where the long process had condensed and was distinguishable from the surrounding mesenchyme, it did indeed appear to be narrowly separated from the stapes.

The stapedius tendon forms from the interhyale, a second-arch condensation which develops in continuity with the stapes but which never becomes cartilaginous (Rodríguez-Vázquez, 2005, 2009). Given that the mesenchymal precursor of the incudal long process condenses out separately from the stapes, a stapedial muscle insertion onto the incudostapedial joint capsule, or onto the long process itself, would most likely result from a migration of fibres following ossicular union. The

presence of such an insertion in a small minority of individuals does not represent strong evidence for a common, second-arch origin of long process and stapes.

Clinical evidence

Abnormalities of the middle ear ossicles have frequently been interpreted in the light of a dual-arch origin of the malleus and incus. Stapes abnormality is quite commonly associated with the absence of the incudal long process (Swartz & Faerber, 1985; Nomura *et al.*, 1988; Park & Choung, 2009), and this has been linked to the supposed second-arch origin of these structures. Other conditions interpreted along similar lines include 'malleus bar', in which there is a bony connection between the manubrium and the posterior tympanic wall (Nomura *et al.*, 1988), 'spindle handle', in which the manubrium and long process of the incus are abnormal (Nomura *et al.*, 1988), and a case featuring bony union between the manubrium and the head of the stapes, with a fibrous long process (Hough, 1963).

Interestingly, prior to the work of Hanson et al. (1959; 1962), Hough (1958) had described a case of 'triple bony union' between manubrium, long process and stapes, and had postulated a number of explanations for the abnormality which assumed a first-arch origin of the malleus and incus. Yamamoto et al. (2014) found that ankyloses of the malleus head or short process of the incus (indisputably first-arch structures) were in 5 of 7 cases associated with malformations of the manubrium, which they noted could not easily be explained in terms of dual-arch origins. Contrary to both developmental hypotheses, it has been argued that the rare condition of congenital, bilateral absence of the incus suggests that the malleus and incus are derived from separate mesenchymal populations (Rahbar *et al.*, 2002). Ossicular malformations are rarely the same between patients (Swartz & Faerber, 1985) and when Cousins & Milton (1988) reviewed a wide range of ossicular abnormalities found in 68 patients, they concluded that the deformities observed could suggest either a first-arch or a dual-arch origin of the incus, depending on the specific case.

We would argue that it is overly simplistic to suppose that each case of ossicular abnormality can be interpreted in the light of pharyngeal arch origins, and conversely that pharyngeal arch origins can be elucidated from a consideration of such abnormalities. Some genes are expressed in more than one pharyngeal arch, and disruptions to them could affect structures with different arch origins. For example, the homeobox gene *Dlx-2* is believed to regulate proximo-distal patterning in both the first and second pharyngeal arches: mice which are homozygous for *Dlx-2* gene mutations have malformations in derivatives of both arches (Qiu *et al.*, 1997). Both incus and stapes are abnormal in these animals, and they often fail to articulate. Even a gene expressed in one arch only could affect the development of other arches, if the molecular communication between adjacent structures were compromised.

Conclusion

The long process of the incus was continuous with the incudal body in all cartilaginous-stage embryos, and the manubrium was continuous with the body of the malleus in all but one. We cannot

explain why there was an apparent partial division between manubrium and upper malleus in one embryo, but it was clearly atypical.

If the manubrium and long process really are second-arch derivatives, this must arise from the apparent continuity between first- and second-arch mesenchyme found at a much earlier embryonic stage, as the Anson group proposed. Based on our examination of serial sections very similar to theirs, we do not believe that future structural boundaries can be reliably determined in embryos this young simply through observation of classically stained sections. This calls into question the main strand of evidence upon which the Anson group's version of the dual-arch interpretation is based. Evidence from the stapedius muscle insertion and from congenital ossicular malformations appears to be very weak. Although we cannot unambiguously reject the dual-arch model of ossicular development, our observations, on balance, favour the classical interpretation.

Given the difficulties in visual identification of first- and second-arch boundaries in very young embryos, it would appear that molecular lineage-tracking techniques are needed in order to provide a definitive answer to the question of ossicular developmental origins. *Hoxa2* is expressed in second-arch mesenchyme, so serial *in situ* hybridisation analysis could allow tracking of the mesenchymal populations over time. Although such studies have not yet been done on human embryos, results from murine studies suggest that all of the incus and most of the malleus (including the manubrium but excluding the goniale and orbicular apophysis) develop from first pharyngeal arch mesenchyme, strongly supporting the classical interpretation. Based on our reconsideration of human embryonic development, we find no compelling reason to disagree with this.

Acknowledgements

The authors would like to thank Matthew R. B. Farr for offering his help and expertise, and Prof. Graham J. Burton for kindly allowing access to the Boyd Collection. We thank the two anonymous reviewers whose comments have helped us to improve the manuscript. This paper arose from an honours dissertation by CMB, sponsored by the Department of Physiology, Development & Neuroscience, University of Cambridge. Additional support came from St. Catharine's College.

References

Amin, S. & Tucker, A.S. (2006) Joint formation in the middle ear: lessons from the mouse and guinea pig. *Developmental Dynamics* **235**: 1326-1333.

Anson, B.J., Hanson, J.R. & Richany, S.F. (1960) Early embryology of the auditory ossicles and associated structures in relation to certain anomalies observed clinically. *Annals of Otology, Rhinology & Laryngology* **69**: 427-447.

Anthwal, N., Joshi, L. & Tucker, A.S. (2013) Evolution of the mammalian middle ear and jaw: adaptations and novel structures. *Journal of Anatomy* **222**: 147–160.

Anthwal, N. & Thompson, H. (2016) The development of the mammalian outer and middle ear. *Journal of Anatomy* **228**: 217-232.

Ars, B. (1989) Organogenesis of the middle ear structures. *Journal of Laryngology and Otology* **103**: 16-21.

Bluestone, C.D., Simons, J.P. & Healy, G.B. (eds) (2014) *Bluestone and Stool's Pediatric Otolaryngology, volume 1, 5th ed*. Shelton: People's Medical Publishing House.

Chapman, S.C. (2011) Can you hear me now? Understanding vertebrate middle ear development. *Frontiers in Bioscience* **16**: 1675-1692.

Chien, W., Northrop, C., Levine, S., Pilch, B.Z., Peake, W.T., Rosowski, J.J. & Merchant, S.N. (2009) Anatomy of the distal incus in humans. *Journal of the Association for Research in Otolaryngology* **10**: 485-496.

Cousins, V.C. & Milton, C.M. (1988) Congenital ossicular abnormalities: a review of 68 cases. *American Journal of Otology* **9**: 76-80.

Frazer, J.E. (1914) The second visceral arch and groove in the tubo-tympanic region. *Journal of Anatomy and Physiology* **48**: 391–408.

Gaupp, E. (1913) Die Reichertsche Theorie (Hammer-, Amboss- und Kieferfrage). *Archiv für Anatomie und Entwickelungsgeschichte (suppl.)* **1912**: 1-416.

Gendron-Maguire, M., Mallo, M., Zhang, M. & Gridley, T. (1993) Hoxa-2 mutant mice exhibit homeotic transformation of skeletal elements derived from cranial neural crest. *Cell* **75**: 1317-1331.

Gleeson, M., Browning, G.G., Burton, M.J., Clarke, R., Hibbert, J., Jones, N.S., Lund, V.J., Luxon, L.M. & Watkinson, J.C. (2008) *Scott-Brown's Otorhinolaryngology, Head and Neck Surgery, 7th ed*. Boca Raton: CRC Press.

Gopen, Q. (2013) *Fundamental Otology: Pediatric & Adult Practice*. New Delhi: Jaypee Brothers Medical Publishers (P) Ltd.

Hanson, J.R., Anson, B.J. & Bast, T.H. (1959) The early embryology of the auditory ossicles in man. *Quarterly Bulletin of Northwestern University Medical School* **33**: 358–379.

Hanson, J.R. & Anson, B.J. (1962) Development of the malleus of the human ear. Illustrated in atlas series. *Quarterly Bulletin of Northwestern University Medical School* **36**: 119–137.

Hanson, J.R., Anson, B.J. & Strickland, E.M. (1962) Branchial sources of the auditory ossicles in man. Part II: observations of embryonic stages from 7 mm. to 28 mm. (CR length) *Archives of Otolaryngology* **76**: 200-215.

Hough, J.V.D. (1958) Malformations and anatomical variations seen in the middle ear during the operation for mobilization of the stapes. *Laryngoscope* **68**: 1337-1379.

Hough, J.V.D. (1963) Congenital malformations of the middle ear. *Archives of Otolaryngology* **78**: 335-343.

Jarvik, E. (1980) *Basic Structure and Evolution of Vertebrates, volume 2*. London: Academic Press.

Kanagasuntheram, R. (1967) A note on the development of the tubotympanic recess in the human embryo. *Journal of Anatomy* **101**: 731–741.

Kitazawa, T., Fujisawa, K., Narboux-Nême, N., Arima, Y., Kawamura, Y., Inoue, T., Wada, Y., Kohro, T., Aburatani, H., Kodama, T., Kim, K.S., Sato, T., Uchijima, Y., Maeda, K., Miyagawa-Tomita, S., Minoux, M., Rijli, F.M., Levi, G., Kurihara, Y. & Kurihara, H. (2015) Distinct effects of *Hoxa2* overexpression in cranial neural crest populations reveal that the mammalian hyomandibular-ceratohyal boundary maps within the styloid process. *Developmental Biology* **402**: 162-174.

Louryan, S. (1993) Le développement des osselets de l'ouie chez l'embryon humain: corrélations avec les données recueillies chez la souris. *Bulletin de l'Association des Anatomistes* **77**: 29-32.

Luo, Z.-X. (2011) Developmental patterns in Mesozoic evolution of mammal ears. *Annual Review of Ecology, Evolution, and Systematics* **42**: 355–380.

Mallo, M. (1997) Retinoic acid disturbs mouse middle ear development in a stage-dependent fashion. *Developmental Biology* **184**: 175-186.

Mallo, M., Schrewe, H., Martin, J.F., Olson, E.N. & Ohnemus, S. (2000) Assembling a functional tympanic membrane: signals from the external acoustic meatus coordinate development of the malleal manubrium. *Development* **127**: 4127-4136.

Mansour, S., Magnan, J., Haidar, H., Nicolas, K. & Louryan, S. (2013) *Comprehensive and Clinical Anatomy of the Middle Ear*. Berlin: Springer-Verlag.

Mason, M.J. (2013) Of mice, moles and guinea-pigs: functional morphology of the middle ear in living mammals. *Hearing Research* **301**: 4-18.

Matsuo, I., Kuratani, S., Kimura, C., Takeda, N. & Aizawa, S. (1995) Mouse Otx2 functions in the formation and patterning of rostral head. *Genes and Development* **9**: 2646-2658.

Minoux, M., Kratochwil, C.F., Ducret, S., Amin, S., Kitazawa, T., Kurihara, H., Bobola, N., Vilain, N. & Rijli, F.M. (2013) Mouse Hoxa2 mutations provide a model for microtia and auricle duplication. *Development* **140**: 4386-4397.

Miyake, T., Cameron, A.M. & Hall, B.K. (1996) Stage-specific onset of condensation and matrix deposition for Meckel's and other first arch cartilages in inbred C57BL/6 mice. *Journal of Craniofacial Genetics and Developmental Biology* **16**: 32-47.

Moody, D. & Lozanoff, S. (1998) SURFdriver: A practical computer program for generating three-dimensional models of anatomical structures using a PowerMac. *Clinical Anatomy* **11**: 132.

Nomura, Y., Nagao, Y. & Fukaya, T. (1988) Anomalies of the middle ear. *Laryngoscope* **98**: 390-393.

O'Gorman, S. (2005) Second branchial arch lineages of the middle ear of wild-type and *Hoxa2* mutant mice. *Developmental Dynamics* **234**: 124-131.

Otto, H.-D. (1984) Der Irrtum der Reichert-Gauppschen Theorie. Ein Beitrag zur Onto- und Phylogenese des Kiefergelenks und der Gehörknöchelchen der Säugetiere. *Anatomischer Anzeiger* **155**: 223-238.

Park, K. & Choung, Y.H. (2009) Isolated congenital ossicular anomalies. *Acta Oto-Laryngologica* **129**: 419-422.

Pasha, R. & Golub, J.S. (2014) *Otolaryngology - Head and Neck Surgery: Clinical Reference Guide, 4th ed*. San Diego: Plural Publishing, Inc.

Presley, R. (1984) Lizards, mammals and the primitive tetrapod tympanic membrane. *Symposia of the Zoological Society of London* **52**: 127-152.

Qiu, M., Bulfone, A., Ghattas, I., Meneses, J.J., Christensen, L., Sharpe, P.T., Presley, R., Pedersen, R.A. & Rubenstein, J.L. (1997) Role of the Dlx homeobox genes in proximodistal patterning of the branchial arches: mutations of Dlx-1, Dlx-2, and Dlx-1 and -2 alter morphogenesis of proximal skeletal and soft tissue structures derived from the first and second arches. *Developmental Biology* **185**: 165-184.

Rahbar, R., Neault, M.W. & Kenna, M.A. (2002) Congenital absence of the incus bilaterally without other otologic anomalies: a new case report. *Ear, Nose, & Throat Journal* **81**: 274-276, 278.

Reichert, C. (1837) Ueber die Visceralbogen der Wirbelthiere im Allgemeinen und deren Metamorphosen bei den Vögeln und Säugethieren. *Archiv für Anatomie, Physiologie und Wissenschaftliche Medicin*: 120-222.

Rijli, F.M., Mark, M., Lakkaraju, S., Dierich, A., Dollé, P. & Chambon, P. (1993) A homeotic transformation is generated in the rostral branchial region of the head by disruption of Hoxa-2, which acts as a selector gene. *Cell* **75**: 1333-1349.

Rodríguez-Vázquez, J.F. (2005) Development of the stapes and associated structures in human embryos. *Journal of Anatomy* **207**: 165-173.

Rodríguez-Vázquez, J.F. (2009) Development of the stapedius muscle and pyramidal eminence in humans. *Journal of Anatomy* **215**: 292-299.

Rodríguez Vázquez, J.F., Mérida Velasco, J.R. & Jiménez Collado, J. (1991) A study of the os goniale in man. *Acta Anatomica* **142**: 188-192.

Sienknecht, U.J. (2013) Developmental origin and fate of middle ear structures. *Hearing Research* **301**: 19–26.

Standring, S., Ellis, H., Healy, J.C., Johnson, D. & Williams, A. (eds) (2005) *Gray's Anatomy: The Anatomical Basis Of Clinical Practice, 39th ed*. Edinburgh Elsevier Churchill Livingstone.

Strickland, E.M., Hanson, J.R. & Anson, B.J. (1962) Branchial sources of auditory ossicles in man. I. Literature. *Archives of Otolaryngology* **76**: 100-122.

Swartz, J.D. & Faerber, E.N. (1985) Congenital malformations of the middle ear: high-resolution CT findings of surgical import. *American Journal of Roentgenology* **144**: 501-506.

Takechi, M. & Kuratani, S. (2010) History of studies on mammalian middle ear evolution: a comparative morphological and developmental biology perspective. *Journal of Experimental Zoology B: Molecular and Developmental Evolution* **314**: 417-433.

Thévenaz, P., Ruttimann, U.E. & Unser, M. (1998) A pyramid approach to subpixel registration based on intensity. *IEEE Transactions on Image Processing* **7**: 27-41.

Thompson, H., Ohazama, A., Sharpe, P.T. & Tucker, A.S. (2012) The origin of the stapes and relationship to the otic capsule and oval window. *Developmental Dynamics* **241**: 1396-1404.

Tucker, A.S., Watson, R.P., Lettice, L.A., Yamada, G. & Hill, R.E. (2004) *Bapx1* regulates patterning in the middle ear: altered regulatory role in the transition from the proximal jaw during vertebrate evolution. *Development* **131**: 1235-1245.

Whyte, J., Cisneros, A., Yus, C., Fraile, J., Obón, J. & Vera, A. (2009) Tympanic ossicles and pharyngeal arches. *Anatomia, Histologia, Embryologia* **38**: 31-33.

Williams, P.L., Warwick, R., Dyson, M. & Bannister, L.H. (eds) (1989) *Gray's Anatomy, 37th ed*. Edinburgh: Churchill Livingstone.

Williams, P.L., Bannister, L.H., Berry, M.M., Collins, P., Dyson, M., Dussek, J.E. & Ferguson, M.W.J. (eds) (1995) *Gray's Anatomy, 38th ed*. Edinburgh: Churchill Livingstone.

Yamamoto, Y., Takahashi, K., Morita, Y., Ohshima, S. & Takahashi, S. (2014) Can the pathogenesis of auditory ossicular malformations be explained by the branchial-based theory? Evaluation by the consecutive distribution of embryologic foci in 87 cases. *Otology & Neurotology* **35**: 449-453.

Figure captions

Figure 1

Diagrammatic illustrations of the left malleus, incus and stapes of an adult human, seen from rostromedially. Potential developmental origins are indicated in colour: blue = first pharyngeal arch origin, cream = second pharyngeal arch origin, orange = intramembranous ossification (goniale). The "classical" interpretation (left) maintains that all of the malleus and incus, apart from the anterior process of the malleus, are first-arch derivatives, whereas the "dual-arch" interpretation (right) maintains that the long process of the incus and the manubrium of the malleus are derived from the second arch. Approximate developmental boundaries within the malleus and incus are drawn after the diagram in Anson et al. (1960). The stapes may be of dual origin (see Introduction), but this is not represented in the diagram. Scale bar 3 mm.

Figure 2

WinSurf reconstructions of the pharynges (pink), left facial nerves (yellow) and left pharyngeal arch mesenchymal derivatives (blue, cream) in embryos of four developmental stages, viewed from laterally and slightly rostrally. The dotted line in the stage A reconstruction represents the approximate position of the boundary between the first and second pharyngeal arches, visible in

some of the original sections as a pale line extending between pharyngeal pouch I (P1) and cleft I (not shown). The condensing second-arch mesenchyme (cream) is visible in the stage B reconstruction. The first-arch mesenchymal condensations (blue) become visible in later stages, but in the stage C embryo the boundaries between first- and second-arch structures are still very difficult to discern. The chorda tympani nerve (CT) divides the developing manubrium of the malleus from the long process of the incus. The stapes is hidden behind the developing incus and hence is not visible in the figures. The stage A reconstruction was of embryo H237 (8.5 mm), stage B was H67 (9.5 mm), stage C was H883 (14.5 mm) and stage E was H973 (16 mm). Scale bar 1 mm.

Key to all figures: A1-2 = mesenchymal condensations within pharyngeal arches I-II; C1 = pharyngeal cleft I; CS = lateral cervical sinus, from where pharyngeal clefts II-IV originate; CT = chorda tympani; EAM = external auditory meatus; HI = head of the incus; HM = head of the malleus; I = incus; IH = interhyale; LH = laterohyale; LP = long process of the incus; M = malleus; MC = Meckel's cartilage (or if precartilaginous, Meckel's bar); MM = manubrium of the malleus; P = pharynx; PW = pharyngeal 'wing' (precursor of tubotympanic recess); P1-4 = pharyngeal pouches I-IV; RC = Reichert's cartilage (or if precartilaginous, Reichert's bar); S = stapes; SB = stapes blastema; TR = tubotympanic recess; TT = tensor tympani muscle; VII = facial nerve.

Figure 3

The development of the external meatus. A: Winsurf reconstruction of a 8.5 mm stage A embryo head (H237), viewed from rostrally and slightly to the right. The original contact between pharyngeal pouch I and cleft I is prominent. B: Photomicrograph of a section through another stage A embryo (RJH31, 7 mm), showing pouch I extending towards cleft I: the pouch endoderm is narrowly in contact with cleft ectoderm. C: Winsurf reconstruction of a 13.5 mm stage C embryo head (H854), viewed from rostrally and slightly to the left. The original contact between pharyngeal pouch I and cleft I is disappearing; the definitive external auditory meatus (EAM) is invaginating rostroventral to this. D: Photomicrograph of a section through the same embryo, showing the vestigial extension of pouch I projecting towards cleft I. E: a more rostral section of the same embryo again, showing the definitive EAM. F: Winsurf reconstruction of a 16 mm stage E embryo (H973), viewed from a dorsal, lateral and rostral position. The original contact between pouch I and cleft I has disappeared; the bases of pouches I and II are united into a wing-like pharyngeal extension. Rostral to this, the definitive EAM continues to invaginate. G: Photomicrograph of a section through the same embryo, showing the EAM. Reconstructions A, C and F are not to scale; facial nerve (yellow) and condensations within the mesenchyme of pharyngeal arches I (blue) and II (cream) are shown on the embryos' left sides only. Scale bar for all photomicrographs 0.5 mm. See Fig. 2 for key.

Figure 4

Photomicrographs of three transverse sections through the ear region of a 9.5 mm embryo (H67, stage B). Section A is the most caudal; part of the stapes blastema (SB) is visible adjacent to the first pouch (P1). The dark mesenchyme between pouch I and cleft I marks the future location of the incus. Section B is around 80 μm rostral to section A: the chorda tympani (CT) has emerged from the facial nerve and is travelling dorsally. The black arrows indicate the position of a pale line which appears to separate arch I (above) from arch II (below). Section C is around 90 μm rostral to section B, in the region where the malleus would develop: the chorda tympani has reached what is likely to be arch I territory, but there is no longer any clear sign of a division between the arches. Scale bar 0.5 mm. See Fig. 2 for key.

Figure 5

Photomicrographs illustrating the development of the malleus in six human embryos, in transverse section. A: 8.5 mm embryo (H237, stage A); B: 13.5 mm embryo (H854, stage C); C: 13.5 mm embryo (H24, stage D); D: 18 mm embryo (H242, stage E); E: 22 mm embryo (H594, stage F); F: 28 mm embryo (H585, stage G). The condensed mesenchyme visible between the first cleft (C1) and the pharynx (P) in panel B represents the beginnings of the malleus, but its boundaries are still very diffuse. Note the clear separation between the developing malleus and the condensing second arch mesenchyme (A2/RC). Scale bar 0.5 mm. See Fig. 2 for key.

Figure 6

Photomicrographs illustrating the development of the incus in the same six human embryos as depicted in Fig. 5. A: 8.5 mm embryo (H237, stage A); B: 13.5 mm embryo (H854, stage C); C: 13.5 mm embryo (H24, stage D); D: 18 mm embryo (H242, stage E); E: 22 mm embryo (H594, stage F); F: 28 mm embryo (H585, stage G). The first signs of an incudal condensation are visible in panel B: in this specimen, the dark band of mesenchymal cells running between cleft I (C1) and pouch I (P1) without any clear interruption is where the long process of the incus will form. The upper part of this band is in arch I territory, the lower part in arch II territory. Scale bar 0.5 mm. See Fig. 2 for key.

Figure 7

Photomicrographs of malleus sections in four of the stage G embryos examined in this study. A: 28 mm embryo (H983); B: 27 mm embryo (H583); C: 29 mm embryo (H988); D: 33.5 mm embryo (H643). Note the line of division, visible as a dark streak, between the head of the malleus and the rest of this ossicle in H983 only. H983 was sectioned in a slightly different plane to the others, which accounts at least in part for the different shape and size of the malleus. See text for further details. Scale bar 0.5 mm. See Fig. 2 for key.

Figure 8

Diagrammatic rostral views of five stages of pharyngeal development in human embryos, based on WinSurf reconstructions; not to scale. The pharynges are curved in these embryos: each opens into the oral and nasal cavities towards the top of the diagram, while at the bottom it tapers into the oesophagus. Derivatives of the first pharyngeal arch mesenchyme are colour-coded blue, derivatives of second pharyngeal arch mesenchyme cream. These are shown, where apparent, on each embryo's left side only. The first and second pharyngeal arch mesenchyme is beginning to condense into ossicular precursors in stage C; just in front of the first pouch, the two mesenchymal populations cannot be separated. The developing stapes is hidden behind the first pouch and first arch derivatives and hence is not visible in the figures. The original contact between pouch I and the caudodorsal end of pharyngeal cleft I is visible in the stage A embryo but later disappears. The external auditory meatus develops as a separate invagination from the rostroventral end of cleft I. See text for a full description of each stage. See Fig. 2 for key.

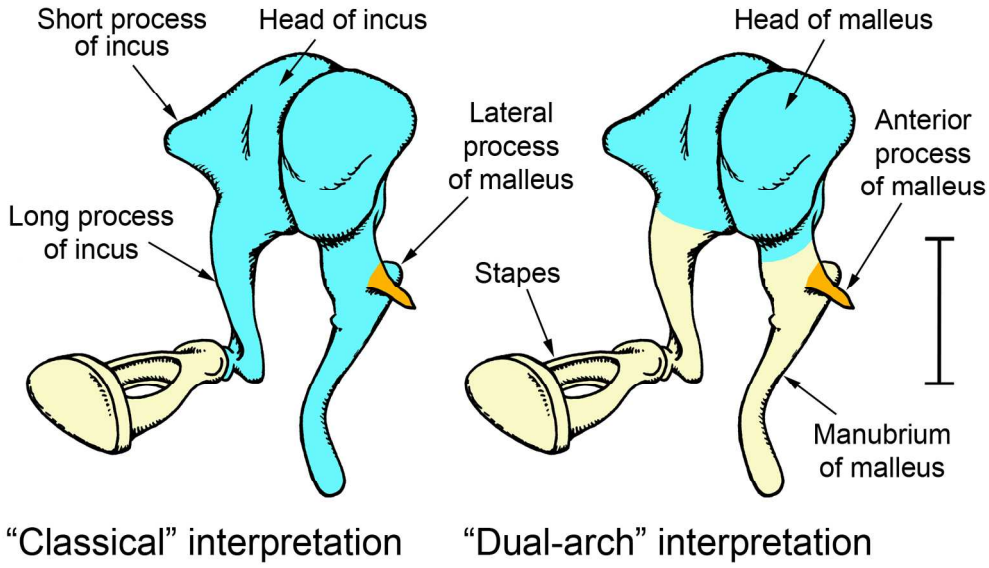

Diagrammatic illustrations of the left malleus, incus and stapes of an adult human, seen from rostromedially. Potential developmental origins are indicated in colour: blue = first pharyngeal arch origin, cream = second pharyngeal arch origin, orange = intramembranous ossification (goniale). The “classical” interpretation (left) maintains that all of the malleus and incus, apart from the anterior process of the malleus, are first-arch derivatives, whereas the “dual-arch” interpretation (right) maintains that the long process of the incus and the manubrium of the malleus are derived from the second arch. Approximate developmental boundaries within the malleus and incus are drawn after the diagram in Anson et al. (1960). The stapes may be of dual origin (see Introduction), but this is not represented in the diagram. Scale bar 3 mm.
165x96mm (300 x 300 DPI)

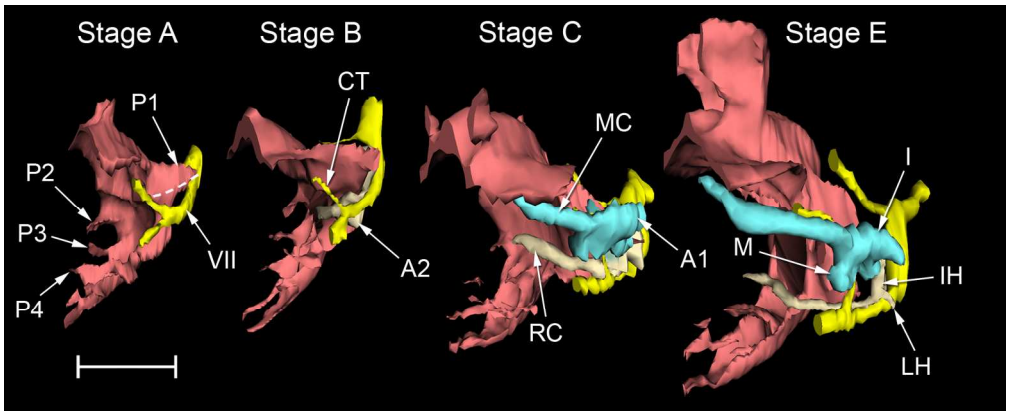

WinSurf reconstructions of the pharynges (pink), left facial nerves (yellow) and left pharyngeal arch mesenchymal derivatives (blue, cream) in embryos of four developmental stages, viewed from laterally and slightly rostrally. The dotted line in the stage A reconstruction represents the approximate position of the boundary between the first and second pharyngeal arches, visible in some of the original sections as a pale line extending between pharyngeal pouch I (P1) and cleft I (not shown). The condensing second-arch mesenchyme (cream) is visible in the stage B reconstruction. The first-arch mesenchymal condensations (blue) become visible in later stages, but in the stage C embryo the boundaries between first- and second-arch structures are still very difficult to discern. The chorda tympani nerve (CT) divides the developing manubrium of the malleus from the long process of the incus. The stapes is hidden behind the developing incus and hence is not visible in the figures. The stage A reconstruction was of embryo H237 (8.5 mm), stage B was H67 (9.5 mm), stage C was H883 (14.5 mm) and stage E was H973 (16 mm). Scale bar 1 mm. Key to all figures: A1-2 = mesenchymal condensations within pharyngeal arches I-II; C1 = pharyngeal cleft I; CS = lateral cervical sinus, from where pharyngeal clefts II-IV originate; CT = chorda tympani; EAM = external auditory meatus; HI = head of the incus; HM = head of the malleus; I = incus; IH = interhyale; LH = laterohyale; LP = long process of the incus; M = malleus; MC = Meckel's cartilage (or if precartilaginous, Meckel's bar); MM = manubrium of the malleus; P = pharynx; PW = pharyngeal 'wing' (precursor of tubotympanic recess); P1-4 = pharyngeal pouches I-IV; RC = Reichert's cartilage (or if precartilaginous, Reichert's bar); S = stapes; SB = stapes blastema; TR = tubotympanic recess; TT = tensor tympani muscle; VII = facial nerve.

165x66mm (300 x 300 DPI)

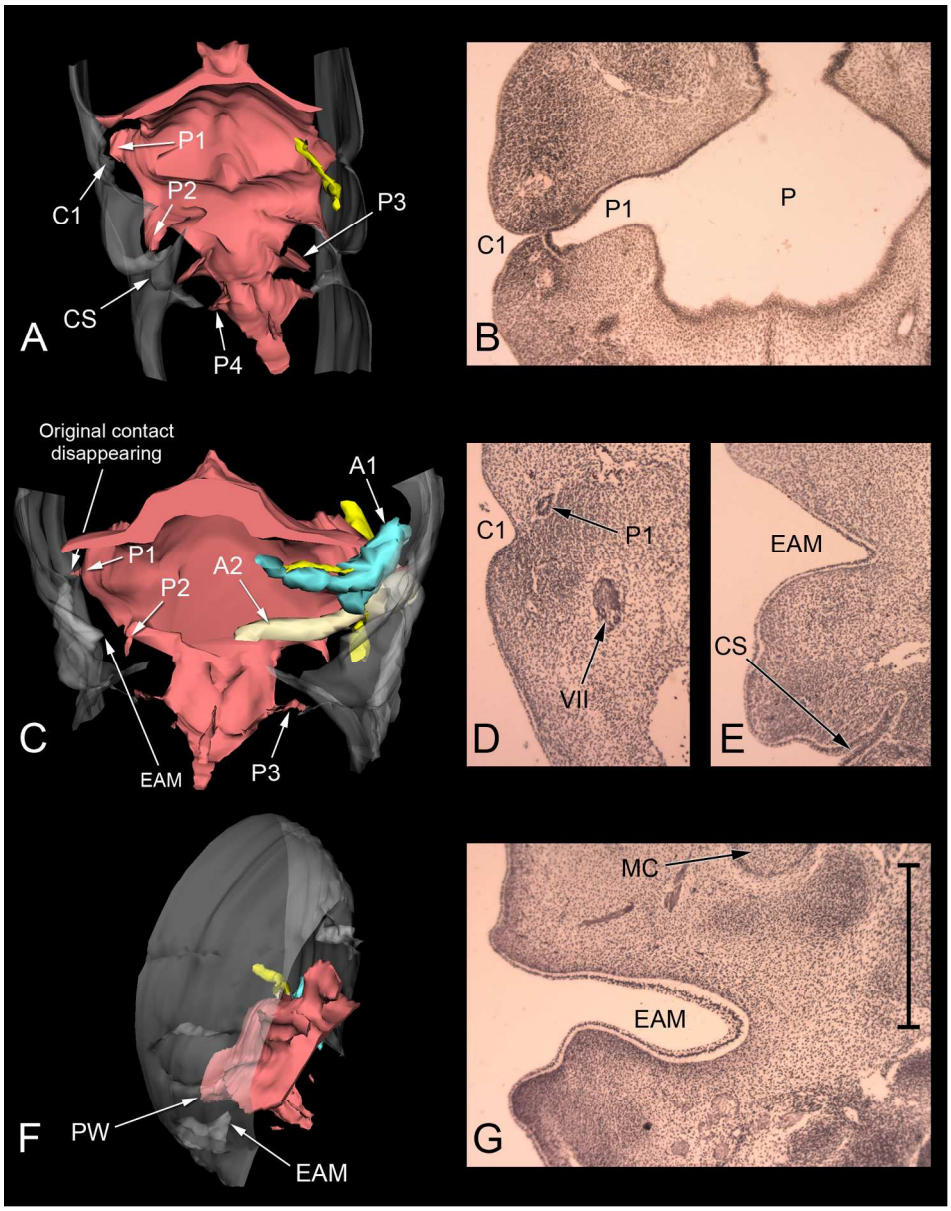

The development of the external meatus. A: Winsurf reconstruction of a 8.5 mm stage A embryo head (H237), viewed from rostrally and slightly to the right. The original contact between pharyngeal pouch I and cleft I is prominent. B: Photomicrograph of a section through another stage A embryo (RJH31, 7 mm), showing pouch I extending towards cleft I: the pouch endoderm is narrowly in contact with cleft ectoderm. C: Winsurf reconstruction of a 13.5 mm stage C embryo head (H854), viewed from rostrally and slightly to the left. The original contact between pharyngeal pouch I and cleft I is disappearing; the definitive external auditory meatus (EAM) is invaginating rostroventral to this. D: Photomicrograph of a section through the same embryo, showing the vestigial extension of pouch I projecting towards cleft I. E: a more rostral section of the same embryo again, showing the definitive EAM. F: Winsurf reconstruction of a 16 mm stage E embryo (H973), viewed from a dorsal, lateral and rostral position. The original contact between pouch I and cleft I has disappeared; the bases of pouches I and II are united into a wing-like pharyngeal extension. Rostral to this, the definitive EAM continues to invaginate. G: Photomicrograph of a section through the same embryo, showing the EAM. Reconstructions A, C and F are not to scale; facial nerve (yellow) and

condensations within the mesenchyme of pharyngeal arches I (blue) and II (cream) are shown on the embryos' left sides only. Scale bar for all photomicrographs 0.5 mm. See Fig. 2 for key.
165x210mm (300 x 300 DPI)

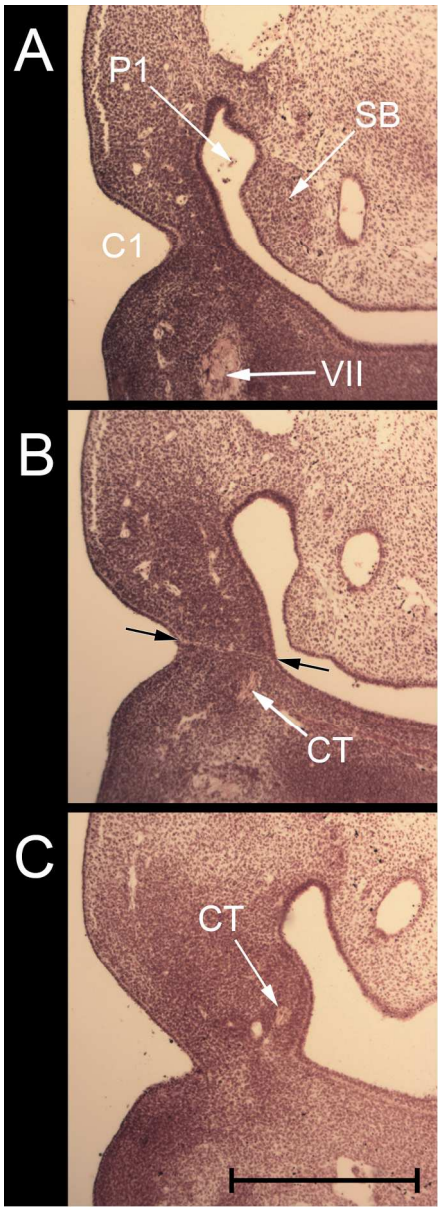

Photomicrographs of three transverse sections through the ear region of a 9.5 mm embryo (H67, stage B). Section A is the most caudal; part of the stapes blastema (SB) is visible adjacent to the first pouch (P1). The dark mesenchyme between pouch I and cleft I marks the future location of the incus. Section B is around 80 μm rostral to section A: the chorda tympani (CT) has emerged from the facial nerve and is travelling dorsally. The black arrows indicate the position of a pale line which appears to separate arch I (above) from arch II (below). Section C is around 90 μm rostral to section B, in the region where the malleus would develop: the chorda tympani has reached what is likely to be arch I territory, but there is no longer any clear sign of a division between the arches. Scale bar 0.5 mm. See Fig. 2 for key.
80x222mm (300 x 300 DPI)

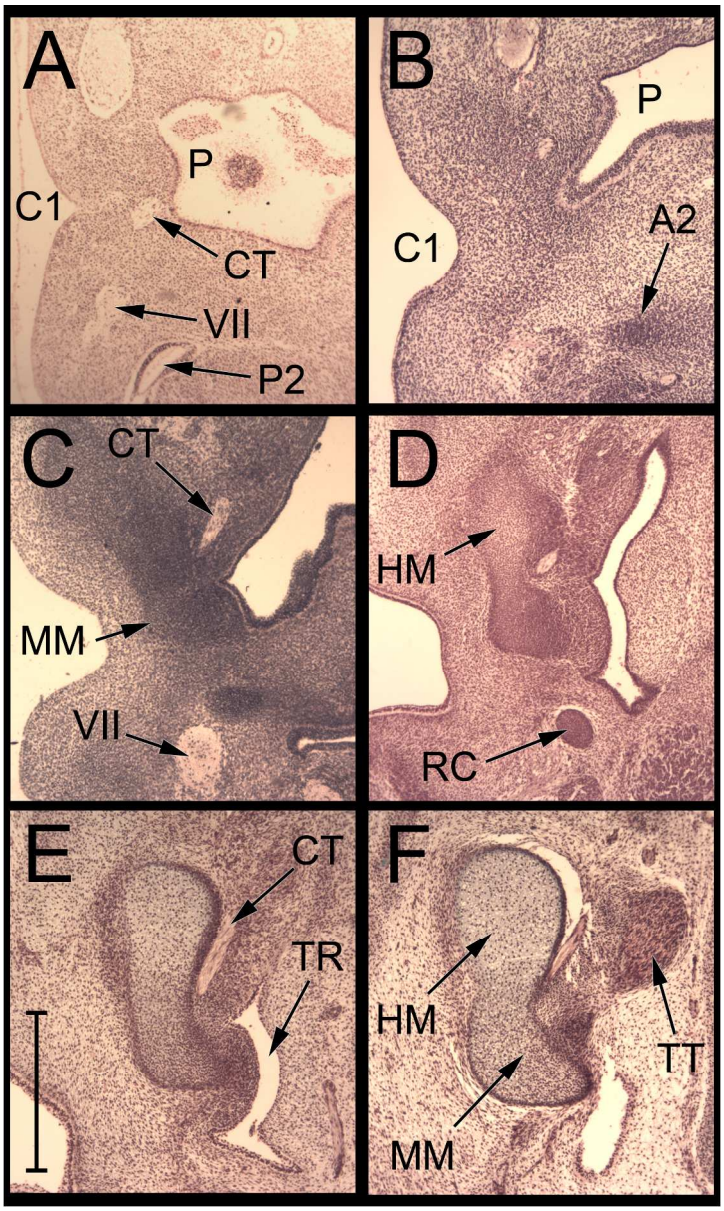

Photomicrographs illustrating the development of the malleus in six human embryos, in transverse section. A: 8.5 mm embryo (H237, stage A); B: 13.5 mm embryo (H854, stage C); C: 13.5 mm embryo (H24, stage D); D: 18 mm embryo (H242, stage E); E: 22 mm embryo (H594, stage F); F: 28 mm embryo (H585, stage G). The condensed mesenchyme visible between the first cleft (C1) and the pharynx (P) in panel B represents the beginnings of the malleus, but its boundaries are still very diffuse. Note the clear separation between the developing malleus and the condensing second arch mesenchyme (A2/RC). Scale bar 0.5 mm. See Fig. 2 for key.
165x276mm (300 x 300 DPI)

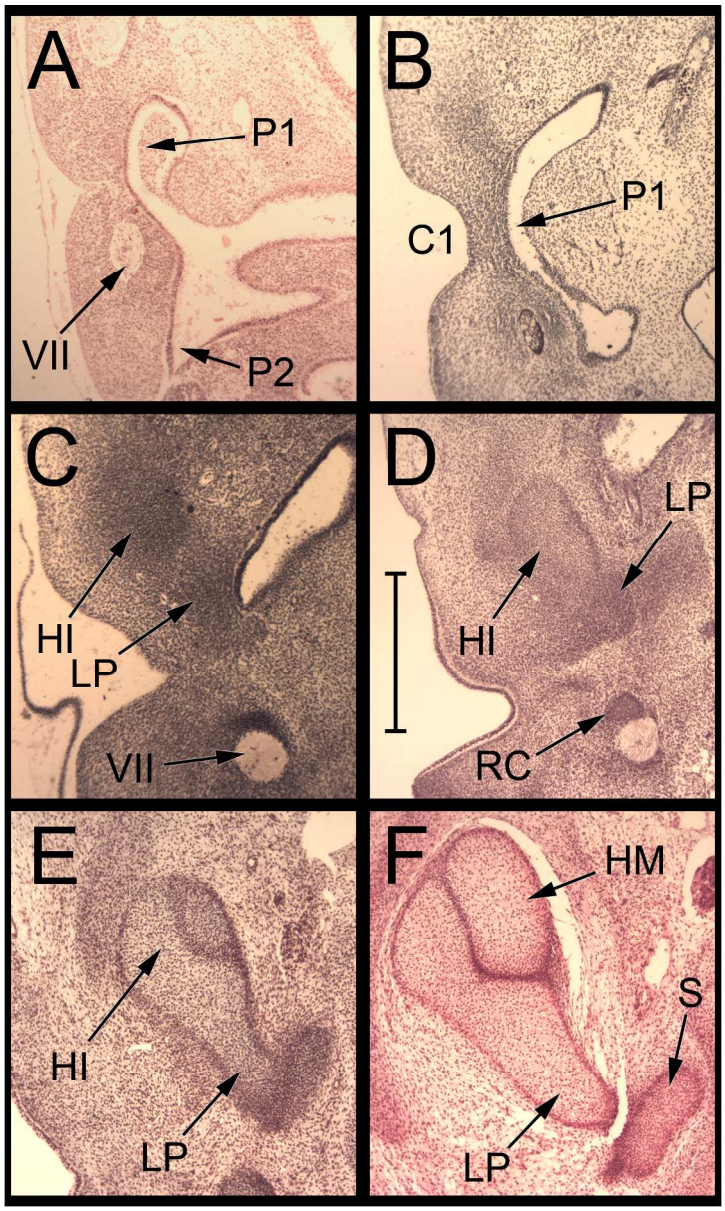

Photomicrographs illustrating the development of the incus in the same six human embryos as depicted in Fig. 5. A: 8.5 mm embryo (H237, stage A); B: 13.5 mm embryo (H854, stage C); C: 13.5 mm embryo (H24, stage D); D: 18 mm embryo (H242, stage E); E: 22 mm embryo (H594, stage F); F: 28 mm embryo (H585, stage G). The first signs of an incudal condensation are visible in panel B: in this specimen, the dark band of mesenchymal cells running between cleft I (C1) and pouch I (P1) without any clear interruption is where the long process of the incus will form. The upper part of this band is in arch I territory, the lower part in arch II territory. Scale bar 0.5 mm. See Fig. 2 for key.
165x275mm (300 x 300 DPI)

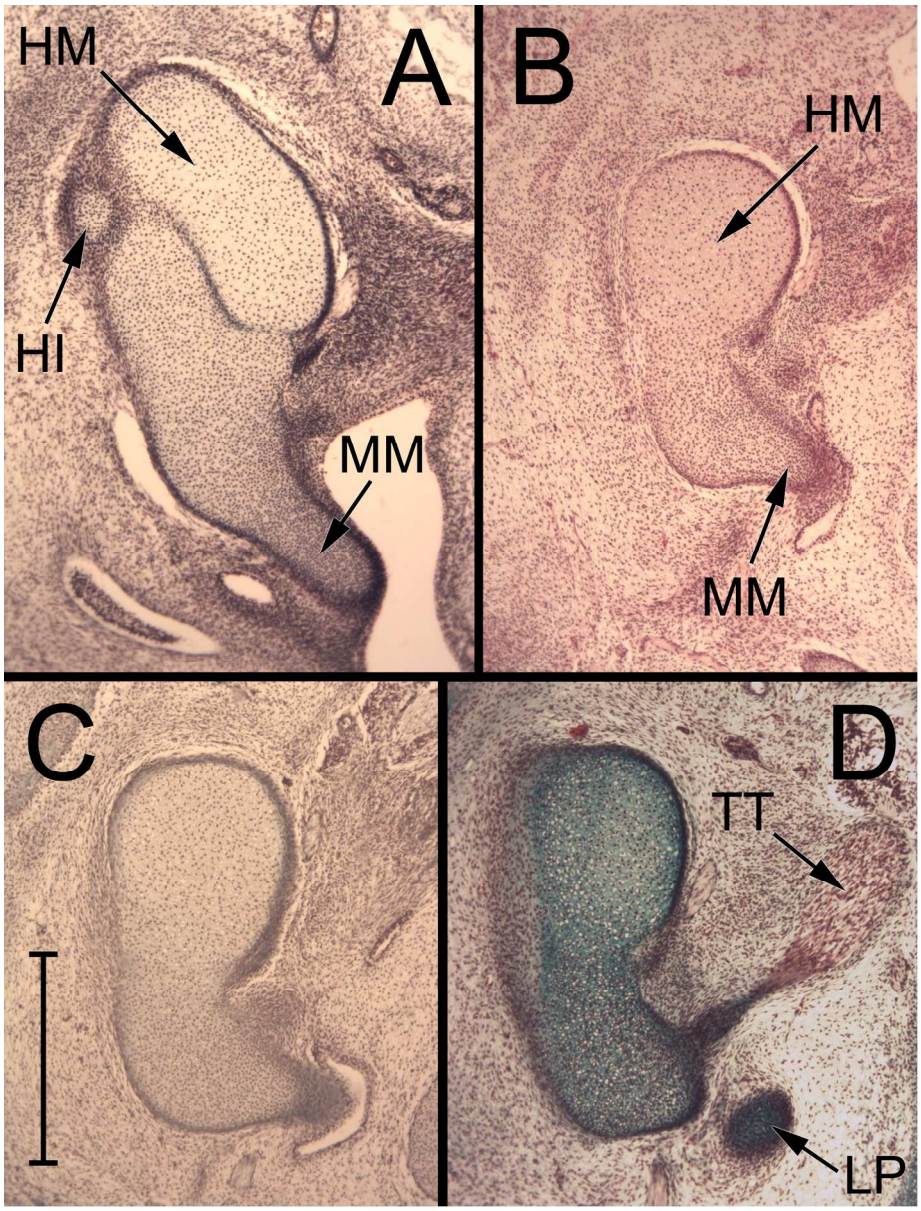

Photomicrographs of malleus sections in four of the stage G embryos examined in this study. A: 28 mm embryo (H983); B: 27 mm embryo (H583); C: 29 mm embryo (H988); D: 33.5 mm embryo (H643). Note the line of division, visible as a dark streak, between the head of the malleus and the rest of this ossicle in H983 only. H983 was sectioned in a slightly different plane to the others, which accounts at least in part for the different shape and size of the malleus. See text for further details. Scale bar 0.5 mm. See Fig. 2 for key.
165x217mm (300 x 300 DPI)

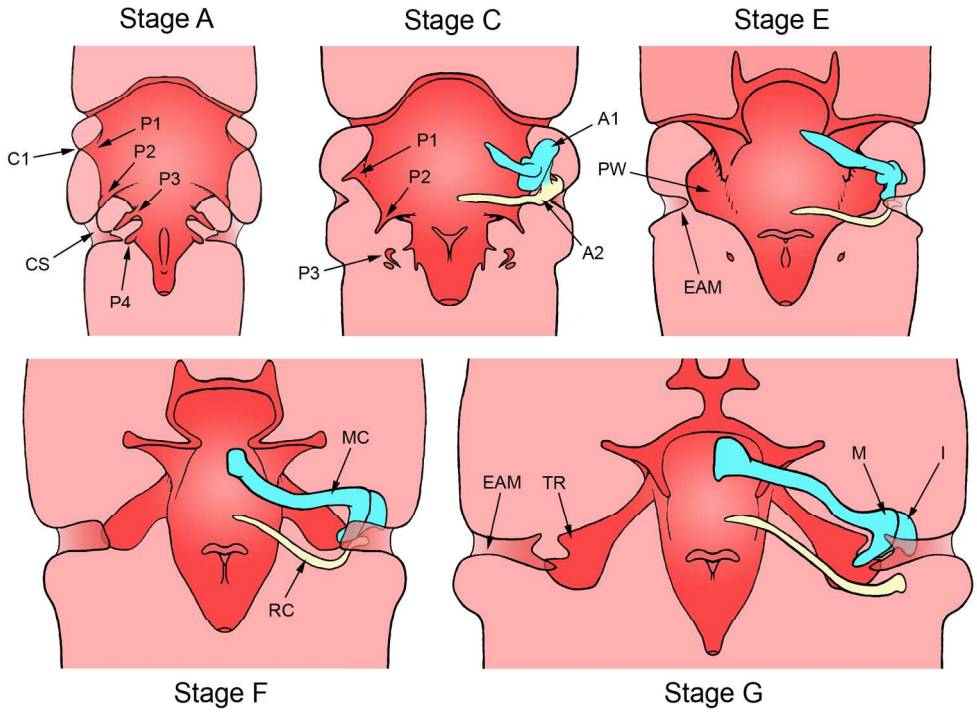

Diagrammatic rostral views of five stages of pharyngeal development in human embryos, based on WinSurf reconstructions; not to scale. The pharynges are curved in these embryos: each opens into the oral and nasal cavities towards the top of the diagram, while at the bottom it tapers into the oesophagus. Derivatives of the first pharyngeal arch mesenchyme are colour-coded blue, derivatives of second pharyngeal arch mesenchyme cream. These are shown, where apparent, on each embryo's left side only. The first and second pharyngeal arch mesenchyme is beginning to condense into ossicular precursors in stage C; just in front of the first pouch, the two mesenchymal populations cannot be separated. The developing stapes is hidden behind the first pouch and first arch derivatives and hence is not visible in the figures. The original contact between pouch I and the caudodorsal end of pharyngeal cleft I is visible in the stage A embryo but later disappears. The external auditory meatus develops as a separate invagination from the rostroventral end of cleft I. See text for a full description of each stage. See Fig. 2 for key.
165x120mm (300 x 300 DPI)

Supplementary table 1

Serially-sectioned embryo specimens from the Boyd Collection examined in this study. Reconstructions were made from a subset of these specimens, as indicated; some of the larger specimens were examined in less detail.

Collection number	Crown-rump length, mm	Middle ear developmental stage (see text for details)	Reconstructions made?
RJH31	7	A	Y
H237	8.5	A	Y
H226	9	A	Y
H67	9.5	B	Y
H116	9-10	B	Y
H33	10	C	Y
H757	10	B	Y
H1026	11	B	Y
RJH53	12	C	Y
H1069	13	C	Y
H24	13.5	D	Y
H854	13.5	C	Y
H186A	14	C	Y
H241	14	E	Y
H533	14	D	Y
H797	14.5	D	Y
H883	14.5	C	Y
H201	15	D	Y
H937	15	C/D	Y
H973	16	E	Y
H25	17	D	Y
H242	18	E	Y
H243	20	F	Y
H916	20	F	Y
H951	20	F	Y
H1106	20	F	Y
H594	22	F	Y
H876	24	G	N
H1103	24	G	Y
H35	25	G	N
H11	26	G	Y
H211	26	G	N
H238	26	G	N
H244	26	G	N
H583	27	G	Y
H585	28	G	Y
H795	28	G	N
H970	28	G	N
H983	28	G	Y
H1022	28.5	G	N
H179	29	G	N
H988	29	G	N
H1061	29	G	N
H31	30	G	N
H209	30	G	N
H910	32.5	G	N
H643	33.5	G	N